Aust. J. Phys., 1989, **42**, 203–13

Infrared Absorption and Reflection Spectra of Crystalline TCNQ Salts

Ajay T. Oza

Department of Physics, Sardar Patel University,
Vallabh Vidyanagar, Gujarat 388120, India.

Abstract

The polarised absorption and reflectance spectra of the three TCNQ salts pyridinium $(TCNQ)_2$, triethylammonium $(TCNQ)_2$ and thermally damaged quinolinium $(TCNQ)_2$ indicate that the absorption features are governed by reflection characteristics. The maximum reflectance curve shows a broad minimum which corresponds to a negative dip in the real part of the dielectric constant and a broad maximum in the imaginary part, as calculated using a Kramers–Kronig analysis. This is ascribed to mobility gaps arising from a frequency-dependent lifetime within the valence band because of the scattering of electrons by $2k_F$ phonons. The exact absorption spectra with all the phonon bands are also analysed and the correlations among the electron–intra-molecular vibration coupling, mobility gaps and the electronic states of charge density waves are discussed.

1. Introduction

The coupling of electronic motion with the phonons associated with intra-molecular vibrations from the optical properties was identified long ago (Kondow and Sakata 1971; Kalpunov *et al.* 1972), but only a few studies have substantiated this problem (Kalpunov *et al.* 1972; Brau *et al.* 1974; Rice *et al.* 1975, 1977; Belousov *et al.* 1976, 1978; Petzelt *et al.* 1979; Rice 1976, 1978; Gutfreund *et al.* 1974). The evaluation of the macroscopic electron–phonon coupling constant using microscopic electron–vibration coupling constants was then successfully attempted (Rice *et al.* 1975, 1977; Rice 1976). The spectra of strongly conducting organic conductors have shown different features (Tanner *et al.* 1977). The observation of the phase oscillations set up by this coupling of charge density waves with the underlying lattice requires a low density of states, which is present in the case of semiconducting TCNQ (7,7,8,8-teracyano-p-quino-dimethane) salts. In the metallic TCNQ salts, the oscillations are buried by freely moving charge carriers.

In the present work, an experimental study and analysis of the absorption and reflectance spectra of three TCNQ salts, namely triethylammonium $(TCNQ)_2$ [$TEtA(TCNQ)_2$], pyridinium $(TCNQ)_2$ [$Py(TCNQ)_2$], and thermally damaged quinolinium $(TCNQ)_2$ [$Qn(TCNQ)_2$], which investigates the details of electron–intra-molecular vibration coupling, is carried out.

2. Experimental

The three TCNQ salts were prepared using standard methods (Acker and

0004-9506/89/020203$03.00

Hertler 1962), with the crystals grown by evaporation from organic solvents (Oza 1980). The conductivities and anisotropies in the conductivities are given in Table 1. The thick black hexagonal plate crystals of $Py(TCNQ)_2$ slowly turned green and finally brown along with continuous distortion into rhombohedral-shaped TCNQ crystals over a long period. $TEtA(TCNQ)_2$ was crystallised in the form of black needles which were also unstable. Soft $Qn(TCNQ)_2$ crystals were heated at 100°C for a few hours so that the surfaces became course and the shapes distorted. These heat damaged crystals were found to have low conductivities (Table 1). The $Qn(TCNQ)_2$ crystals are metallic but the radiation damaged crystals were not strongly conducting (Devereux *et al.* 1980).

Table 1. Electrical conductivities (in $\Omega^{-1}\,m^{-1}$) of the TCNQ salts

Salt	$\sigma_{\parallel}$	$\sigma_{\perp}$	σ_{max}[A]
$TEtA(TCNQ)_2$	400	0·125	$3\cdot7\times10^{4}$
$Py(TCNQ)_2$	2·5	3×10^{-2}	$1\cdot8\times10^{4}$
$Qn(TCNQ)_2$	80	0·2	—
$Qn(TCNQ)_2$[B]	4	3×10^{-3}	$2\cdot7\times10^{4}$

[A] Maximum optical conductivity corresponding to the low frequency envelope.
[B] Damaged by heat.

The needle-shaped crystals of $TEtA(TCNQ)_2$ and $Py(TCNQ)_2$ were arranged without a gap in a plane and glued to two thin parallel fibres for support. A thermally damaged flake of $Qn(TCNQ)_2$ having minimum conductivity along the direction normal to the flat surface was used for the study. Infrared spectrophotometers (Carl Zeiss Jena and Perkin Elmer) with filters, detectors and bright infrared source were used with a polariser for obtaining the absorption and reflectance spectra between 10^{14} and 10^{13} Hz; the resolutions were about $\pm5\ cm^{-1}$. Both NaCl and KBr plates were used as transmitting media for obtaining the absorption spectra over the complete infrared range. The light was polarised such that the electric field vector remained parallel to the strongly conducting direction of the crystals.

3. Results and Discussion

Eight fundamental vibrational modes of the TCNQ molecule which lie below $1\cdot2\times10^{14}$ Hz ($4000\ cm^{-1}$) are observed in the polarised reflectance and absorption spectra of the three TCNQ salts (see Figs 1 and 2). In total there are ten fundamental symmetric a_g vibrational modes of TCNQ, two of which lie at frequencies lower than $1\cdot2\times10^{13}$ Hz ($400\ cm^{-1}$) and two which lie higher than $4\cdot8\times10^{13}$ Hz ($1600\ cm^{-1}$) (Lunelli and Pecile 1970; Kral 1977). Two bands at about $6\cdot7\times10^{13}$ and $9\cdot1\times10^{13}$ Hz (2200 and $3000\ cm^{-1}$) are marked only because of the free electronic motion screening the vibrations. All of these phonon bands are unexpected in the spectra, polarised in the direction of the conducting stacks of TCNQ salts. The bands corresponding to these bare vibrational modes were found to be absent in the direction perpendicular to the molecular stacks, but were also unexpectedly present in the stacking direction in an earlier study (Kondow and Sakata 1971; Kalpunov *et al.* 1972). The reason was explained by Rice (1976) in a model of coupling of electronic motions associated with the electronic conduction in the stacking direction

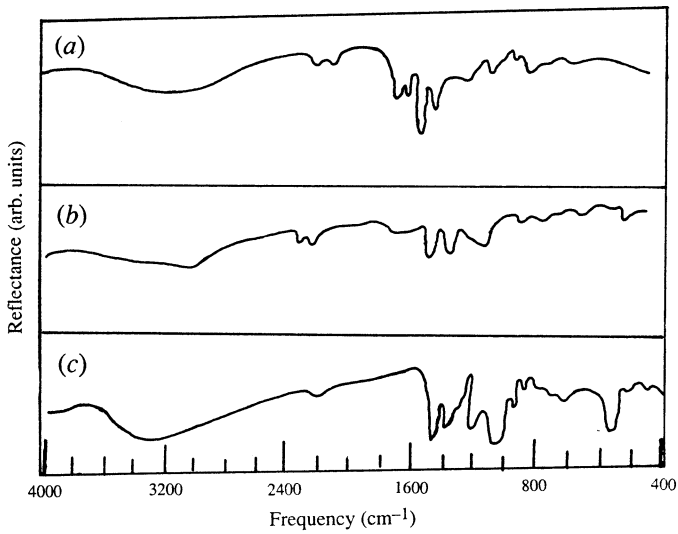

Fig. 1. Reflectance spectra of (*a*) $TEtA(TCNQ)_2$, (*b*) $Py(TCNQ)_2$ and (*c*) $Qn(TCNQ)_2$.

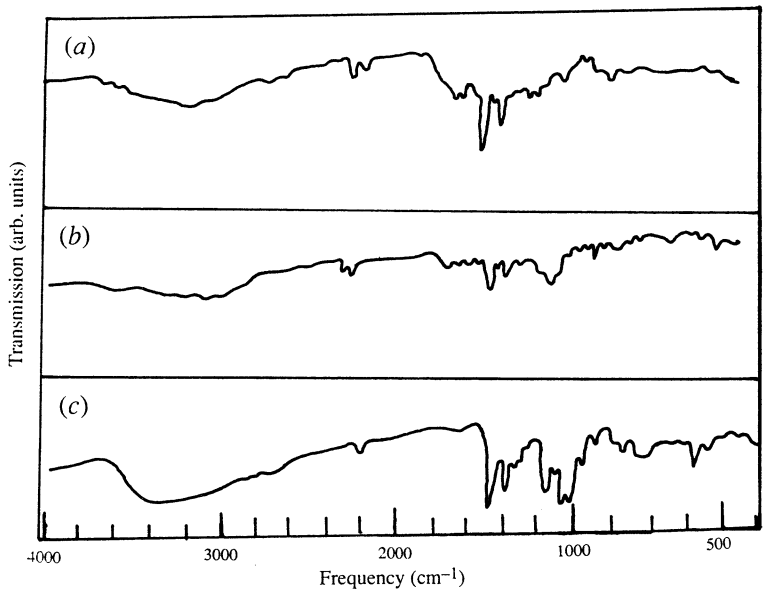

Fig. 2. Absorption spectra of (*a*) $TEtA(TCNQ)_2$, (*b*) $Py(TCNQ)_2$ and (*c*) $Qn(TCNQ)_2$.

with the intra-molecular vibrations. This microscopic model was also found to be successful in calculating the total electron–phonon coupling constant using infrared reflectance spectra (Rice *et al.* 1975, 1977).

Overlooking the phonon bands produced by a_g vibrations, the bases (bottoms) of the bands in the reflectance spectra are joined and these maximum reflectance curves, shown in Fig. 3, indicate a flat depression in reflectance in the infrared range in each case. The maximum reflectance curve passes through the top

points of any dip in reflectance, i.e. representing an increase in transmission. This has physical significance. Although inorganic metal chain complexes and organic quasi-one-dimensional conductors have several identical properties, and in both types of system charge density waves are present, the distinction lies in the waveform or microscopic construction of the charge density waves. In organic conductors, there is a coupling of free electrons with acoustic

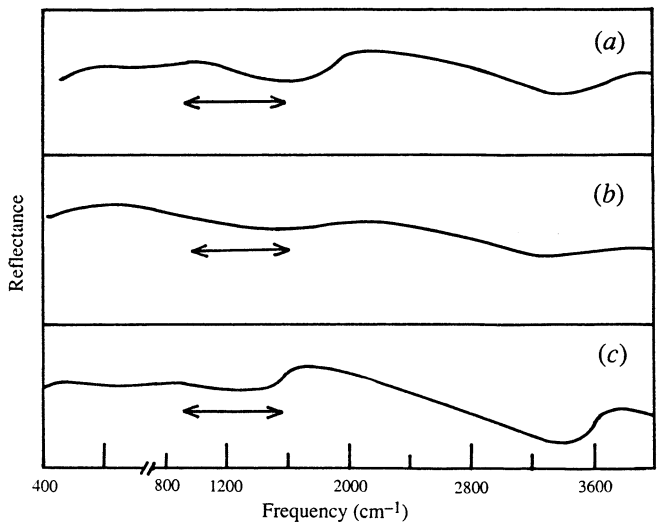

Fig. 3. Maximum reflectance curves for (*a*) $TEtA(TCNQ)_2$, (*b*) $Py(TCNQ)_2$ and (*c*) $Qn(TCNQ)_2$.

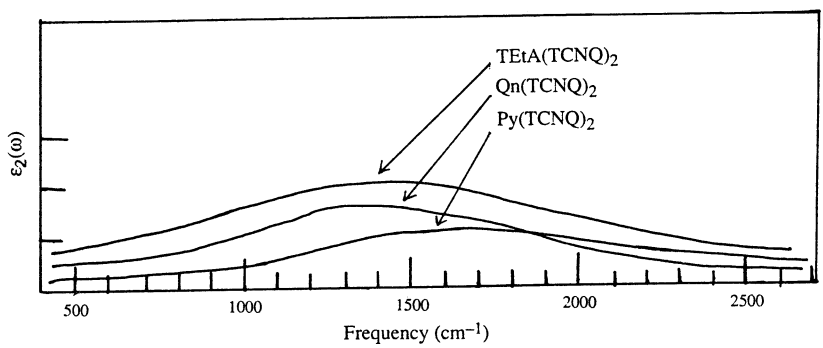

Fig. 4. Imaginary part of the dielectric constant $\epsilon_2(\omega)$ as a function of frequency for the three TCNQ salts.

phonon modes, as well as with the optical phonon modes corresponding to the intra-molecular vibrations. In the donor and acceptor molecules, there are several stretching, deformation, and rotational vibrations while in the metal chain compounds, especially those such as $K_2Pt(CN)_4Br_{0.3}{-}3H_2O$ and $Ir(CO)_{2.9}Cl_{1.1}$, the relative group vibrations of $Pt(CN)_4^{2-}$ or $Ir(CO)_{2.9}Cl_{1.1}$ are considered as a whole in the acoustic modes and the charge carriers

delocalised along the metal chains do not separately couple with C–N or C–O stretching vibrations, but couple with these group vibrations. Thus, the infrared spectra of the inorganic conductors (except the organometallic ones with large ligands) are almost featureless. Therefore, overlooking the phonon bands here is equivalent to considering only acoustic phonon bands broadened by coupled charge carriers and transitions across the resulting Peierls gap and discarding the optical phonon spectrum. This depression is associated with a Peierls transition as in the case of $K_2Pt(CN)_4Br_{0\cdot3}.3H_2O$ (Bruesch 1974). This broad depression when examined with a Kramers–Kronig analysis indicates a broad maximum in the imaginary part of the dielectric constant, i.e. in the $\epsilon_2(\omega)$ spectrum (Fig. 4). The peaks in the range $3\cdot6\times10^{13}$ to $4\cdot8\times10^{13}$ Hz (1200–1600 cm^{-1}) show a deviation from free electron behaviour. The mean free path of the charge carriers is limited by the localisation occuring mainly because of an intrinsic mechanism such as electron–phonon coupling (Bruesch 1974). Strong $2k_F$ scattering leads to nesting of the Fermi surface corresponding to a weak pseudo-potential at high temperatures which results in an energy gap due to a Peierls transition at low temperatures. The scattering of charge carriers by $2k_F$ phonons leads to a modified Drude behaviour with a frequency-dependent lifetime creating a mobility gap (Bruesch 1974). This will be discussed in detail later.

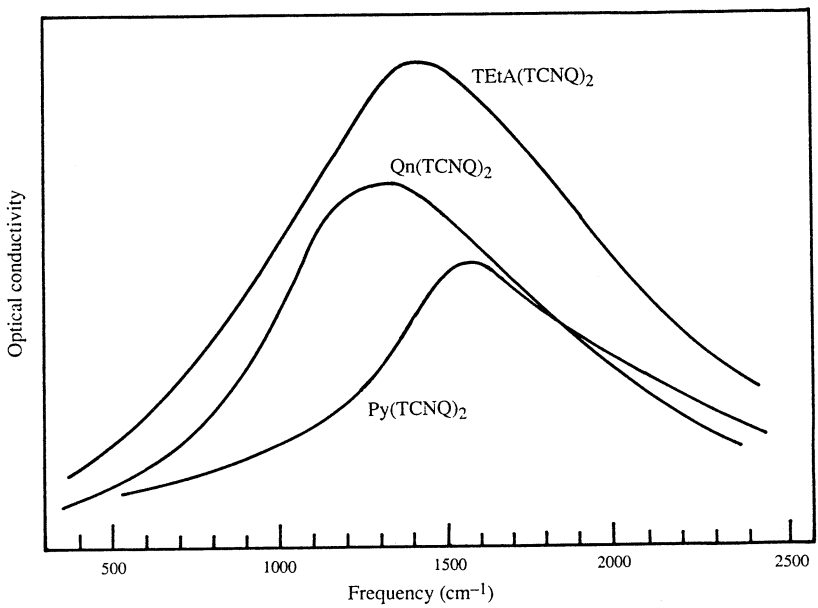

Fig. 5. Optical conductivity peaks in the infrared range for the three TCNQ salts.

The real part of the dielectric constant $\epsilon_1(\omega)$ is found to be very low and remains negative in the range around $4\cdot3\times10^{13}$ Hz giving rise to a highly attenuated total reflectance. [The spectrum of $\epsilon_1(\omega)$ is not shown here.] The optical conductivity $\sigma(\omega) = \epsilon_2(\omega)/4\pi$ is plotted for each TCNQ salt in Fig. 5 and shows strong dispersion with a peak that can be ascribed to the electronic transitions across the Peierls gap (Bruesch 1974). The maximum optical

conductivity calculated from the reflectance spectra increases for these three salts as shown in Table 1. This shows that the charge carriers contributing to the a.c. conductivity in the Peierls semiconducting phase are borrowed from the charge carriers contributing to the d.c. conductivity.

The real transition temperatures of $TEtA(TCNQ)_2$ and $Py(TCNQ)_2$ are considered to be at or slightly above room temperature and for $Qn(TCNQ)_2$ to be around 250 K. At high temperatures where $TEtA(TCNQ)_2$ and $Py(TCNQ)_2$ are unstable, these salts are metallic and all phonon bands in the infrared range are buried under broad and intense electronic absorption bands (II). Here it is assumed that the measured d.c. conductivities of the semiconducing phases are proportional to the conductivities of the metallic phases. The assumption is reasonable because the three organic conductors belong to the same class, i.e. with closed-shell donors and the same acceptor TCNQ forming segregated stacks along which most electronic conduction takes place. Therefore, under a Peierls transition along the TCNQ stacks, almost an equal fraction of charge carriers will be localised or have low mobility, which should be subtracted from the density of the charge carriers in the metallic phase. Thus, as the conductivity of a metallic phase is greater, the corresponding conductivity of the semiconducting phase attained by a Peierls transition is also more in a series of radical–ion salts. This is related to the fact that the a.c. conductivity increases below the Peierls transition temperature at the expense of d.c. conductivity (Heeger 1974).

A comparison of the absorption spectra, obtained with a transmission-type spectrophotometer (Fig. 2), with the reflectance spectra (Fig. 1) immediately reveals that the absorption features are governed by reflection characteristics. This shows that the light absorbed by the inter-molecular vibrations is re-emited when there are de-excitations which occur without any secondary absorption or emission processes, i.e. the singularities of the primary absorption only determine the singularities of the reflectance or transmittance and there are no additional mechanisms which determine bands in the reflectance spectra. Therefore, the absorption spectra in Fig. 2 have all the characteristic bands of the reflectance spectra obtained in the present work and in earlier work (Kondow and Sakata 1971; Kalpunov *et al.* 1972; Brau *et al.* 1974; Petzelt *et al.* 1979). In the absorption spectra, there are sharp bands for frequencies $<1600\ cm^{-1}$ and there are broad and intense bands for higher frequencies. The range 9×10^{13} down to $4\cdot8\times10^{13}$ Hz corresponds to the energy gaps of the Peierls semiconducting phase.

The optical conductivity spectra calculated using a Kramers–Kronig analysis of the reflectance spectra in Fig. 1 are shown in Fig. 6. Since the optical conductivity σ is directly related to the absorption coefficient α according to $\sigma = n_1 \alpha c/4\pi$, where n_1 is the real part of the complex refractive index, and since $n_1(\omega)$ is a weak and monotonic function of frequency, the spectra of $\sigma(\omega)$ and $\alpha(\omega)$ are comparable. The bands in Fig. 6 are numbered for such a comparison. The Kramers–Kronig analysis and calculation of the optical conductivity for $TEtA(TCNQ)_2$ crystals has also been carried out in earlier studies (Kalpunov *et al.* 1972; Brau *et al.* 1974).

In the optical conductivity spectra the sharp bands below the frequency $E_g/\hbar$ are found to be at frequencies 10% lower than those for free TCNQ (Oza

1980; Devereux *et al.* 1980), as expected in the model due to Rice (1976). There are two bands above $E_g/\hbar$ which are only marked in a continuous absorption envelope (Figs 1 and 6).

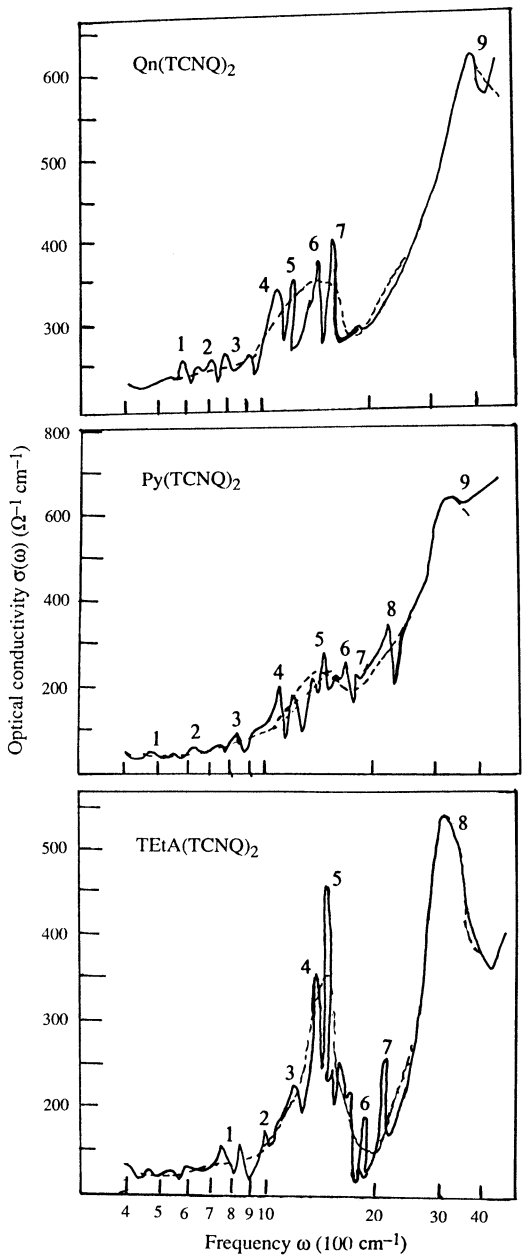

Fig. 6. Optical conductivity calculated with a complete Kramers–Kronig analysis.

For $\omega < E_g/\hbar$ the sharp bands of vibrations of the TCNQ molecule lying at slightly lower frequencies are due to the collective modes of the molecular

lattice and charge distortion, with the bandwidths limited by the natural width of the original phonon states. The additional phase oscillations of the charge density waves, generated by the distortion induced potential of the molecular lattice (which is regularly distorted by the charge density waves themselves in the presence of electron–phonon coupling), are responsible for setting up these optically active collective modes. Even in the absence of electron–phonon coupling, charge density waves (CDW) of wavevector $2k_F$ are generated with periodic potential by this mechanism, and there can be an energy gap due only to this molecular distortion and which can be identified with the Fröhlich CDW state in the model (Rice 1976). There is a change in the polarisation of the bands due to this coupling, the vibrations are activated normal to the molecular plane by the electronic motions, and the mean free paths of the electronic motion are governed by the intra-molecular vibrations.

For $\omega > E_g/\hbar$ these collective modes are damped by electron–hole pair excitations and the damped modes give rise to only identations of the phonon bands in the continuous free electron absorption envelope. The charge carriers with long mean free paths in the bottom of the conduction bands screen the response of the vibration-trapped charge carriers.

The CDW is a collective mode of the electronic charge density in a partially filled band, induced by the low frequency longitudinal acoustic phonon mode of inter-molecular vibrations, unless a gap opens due to a Peierls transition. In the Peierls semiconducting phase the CDW is split into two modes—one lying in the conduction band and the other in the valence band (Fig. 7*a*). The mode in the conduction band is induced in the absence of any electron–phonon coupling by the potential due to the underlying distortion of the molecular lattice. This mode is subjected to pinning–depinning due to imperfections, applied fields and interchain locking and gives rise to a low-frequency far-infrared response. The mode in the valence band becomes adjusted to the lattice due to commensurability or to the high-frequency intra-molecular vibrations induced by this electron–optical phonon coupling. The electronic density inside the valence band oscillates with the frequencies of the intra-molecular vibrations at wavevector $2k_F$ and gives rise to the infrared response. This picture is similar to the Balseiro–Felicov (1980) model. Each mode can further split into A_+ and A_- modes (Rice 1976; Bruesch 1974; Lee *et al.* 1974). The coupling interactions with the underlying vibrations remove the degeneracy of some of the overlapping electronic levels in the valence band. The bandwidths of the quasi-localised levels or narrow bands are determined by the bandwidths of the bare vibrational modes. These bands are narrow because the optical phonons do not have strong dispersion like the acoustic phonons (Fig. 7*b*). The bands are shifted to lower energies by 10% due to electron–intra-molecular vibration coupling. At intermediate energies, these are mobility gaps in the valence band.

The CDWs of low frequency determined by the longitudinal acoustic mode of wavevector $2k_F$ are demodulated with high-frequency optical phonons of wavevector $2k_F$. Thus, the condensed electrons in the CDW face a distorted stair-like potential, leading to distortion of the CDW as shown in Fig. 7*c*. Therefore, the intra-molecular vibrations provide an additional scattering mechanism, resulting in a frequency-dependent lifetime of electrons in a collective mode.

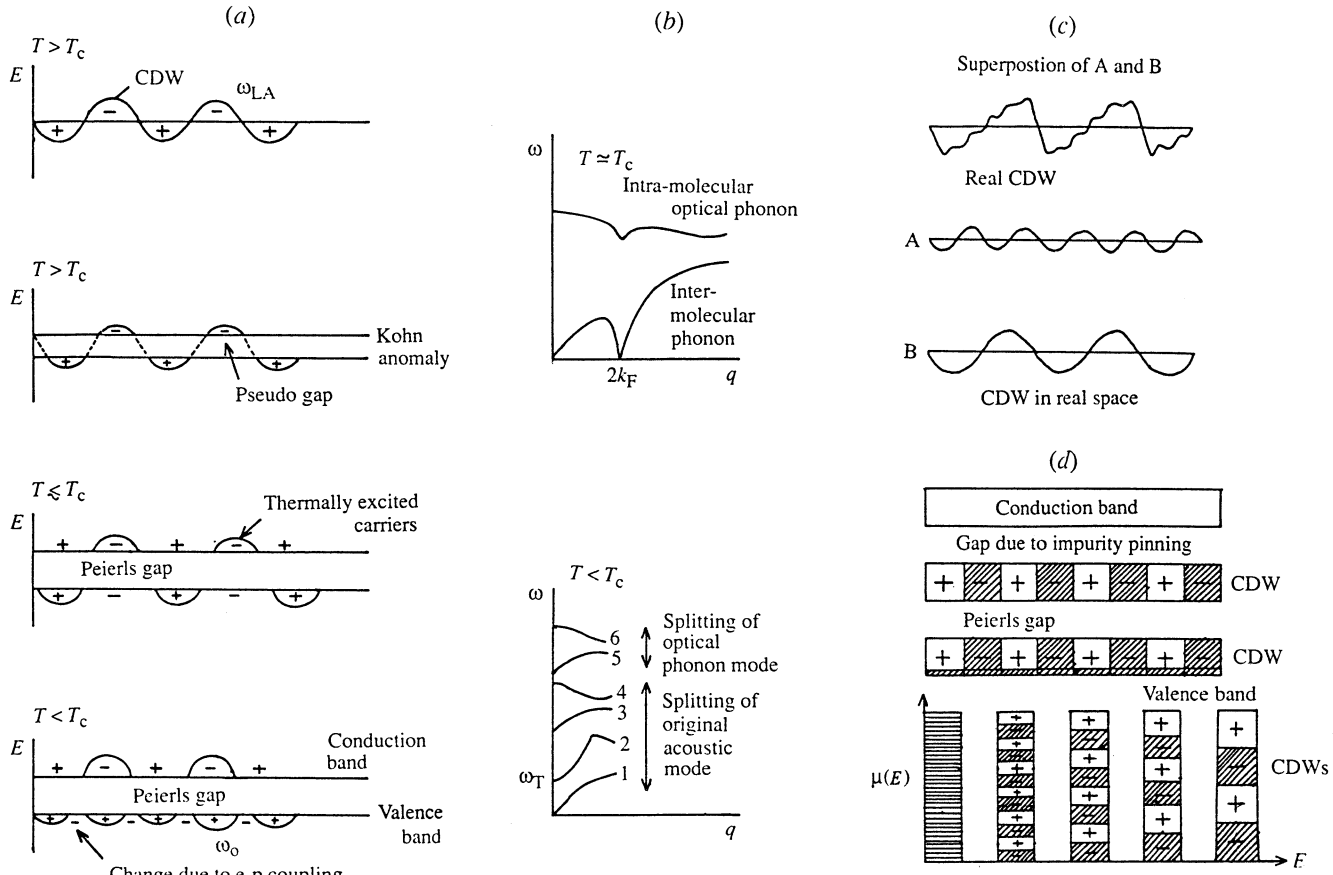

Fig. 7. (*a*) Conduction and valence band modes of the charge density waves. (*b*) Softening of acoustic and optical phonons of wavevector $2k_F$. (*c*) Superposition of two modes having a staircase-like potential. (*d*) Energy levels of CDW.

It can be seen in Fig. 6 that the spectra can be approximated by a two classical oscillator fit for each of the three TCNQ salts (see Table 2). Instead of fitting the approximate bare electronic absorption bands by smoothing the $\sigma(\omega)$ curve, as carried out elsewhere, a graphical method is adopted here in which the inflection points of the conductivity bands (resonance–antiresonance spikes) are joined, as shown by the dashed curves in Fig. 6. These inflection points correspond to the positions of the maxima of the absorption band in the original spectra (Fig. 1). The high-frequency band of this free electron absorption envelope has a low-frequency tail arising from the coupling of the passive bare vibrational model with the broad electronic band. The low-frequency band can be compared with the optical conductivity peak obtained by the Kramers–Kronig analysis of the maximum reflectance curve (Fig. 5). This shows that polarised absorption spectra are direct measures of the optical conductivity spectra rather than reflectance spectra, and that the Kramers–Kronig analysis can be avoided if the optical conductivities are directly calculated from the absorption coefficients.

Table 2. Parameters of the electronic absorption envelopes

Salt	Low-frequency envelope			High-frequency envelope		
	Max. absorption	Central frequency (Hz)	Band-width (Hz)	Max. absorption	Central frequency (Hz)	Band-width (Hz)
$TEtA(TCNQ)_2$	52%	$4{\cdot}2\times10^{13}$	$1{\cdot}65\times10^{11}$	43%	$9{\cdot}3\times10^{13}$	$3{\cdot}15\times10^{13}$
$Py(TCNQ)_2$	42%	$3{\cdot}9\times10^{13}$	$1{\cdot}8\times10^{11}$	61%	$9{\cdot}6\times10^{13}$	$5{\cdot}4\times10^{13}$
$Qn(TCNQ)_2$[A]	70%	$4{\cdot}65\times10^{13}$	$1{\cdot}35\times10^{11}$	31%	$9{\cdot}6\times10^{13}$	$4{\cdot}2\times10^{13}$

[A] Damaged by heat.

Some of the vibrational bands in phenoxazine-iodine and phenothiazine-iodine are also found to broaden and become symmetric because of electron–intramolecular vibration coupling (Oza 1984). On the other hand, in some of the organic semiconductors (Oza 1982, 1983) which are not semiconducting due to a Peierls-type transition, the infrared spectra reveal different kind of features. However, a slightly different type of electron–vibration coupling is encountered in organic polyiodide chain complexes (Mulazzi *et al.* 1981; Oza 1986).

Acknowledgments

The author is thankful to the National Council of Educational Research and Training (NCERT) and the Department of Science and Technology for providing a National Science Talent Scholarship and financial aid respectively. The author would also like to thank the Center of Instrumentation and Service Laboratories (CISL) staff of the Indian Institute of Science, Bangalore, for providing the absorption spectra and Dr G. Venketesh, Ahmedabad Textile Industries Research Association Laboratories, for allowing the measurement of the reflectance spectra.

References

Acker, D. S., and Hertler, W. R. (1962). *J. Am. Chem. Soc.* **84**, 3370.

Balseiro, C. A., and Felicov, L. M. (1980). *Phys. Rev. Lett.* **45**, 662.

Belousov, M. V., Vainrub, A. M., and Vlasova, R. M. (1976). *Fiz. Tverd. Tela (Leningrad)* **19**, 2637.

Belousov, M. V., Vainrub, A. M., Vlasova, R. M., and Semkin V. N. (1978). *Fiz. Tverd. Tela (Leningrad)* **20**, 107.
Brau, A., Bruesch, P., Farges, J. P., Hinz, W., and Kuse, D. (1974). *Phys. Status Solidi* B **62**, 615.
Bruesch, P. (1974). Proc. German Phys. Soc. Conf. on One-dimensional Conductors, Saarbruken, July 1974, Lecture Notes in Physics, Vol. 34 (Ed. H. G. Schuster), p. 194 (Springer: Berlin).
Devereux, F., Neschtschein, M., and Grüner, G. (1980). *Phys. Rev. Lett.* **45**, 53.
Gutfreund, H., Horovitz, B., and Bruesch, P. (1974). *J. Phys.* C **7**, 383.
Heeger, A. J. (1974). Proc. German Phys. Soc. Conf. on One-dimensional Conductors, Saarbruken, Lecture Notes in Physics, July 1974, Vol. 34 (Ed. H. G. Schuster), p. 151 (Springer: Berlin).
Kalpunov, M. G., Panova, T. P., and Borodko, V. G. (1972). *Phys. Status Solidi* A **13**, 1267.
Kondow, T., and Sakata, T. (1971). *Phys. Status Solidi* **6**, 551.
Kral, K. (1977). *Chem. Phys.* **23**, 234.
Lee, P. A., Rice, T. M., and Anderson, P. W. (1974). *Solid State Commun.* **14**, 703.
Lunelli, B., and Pecile, C. (1970). *J. Chem. Phys.* **52**, 3375.
Mulazzi, E., Pollini, J., Piseri, L., and Tubino, R. (1981). *Phys. Rev.* B **24**, 3555.
Oza, A. T. (1980). Ph.D. Thesis, Indian Institute of Science, Bangalore.
Oza, A. T. (1982). *Sardar Patel University Res. J.* **1**, 107.
Oza, A. T. (1983). *Czech. J. Phys.* **23**, 1148.
Oza, A. T. (1984). *Mol. Cryst. Liq. Cryst.* **104**, 377.
Oza, A. T. (1986). *Thin Solid Films* **142**, 153.
Petzelt, J., Kral, K., Rysava, N., Dobiasova, L., Kroupa, J., Oswald, J., Szyskowskii, A., and Graja, A. (1979). *Solid State Commun.* **32**, 1315.
Rice, M. J. (1976). *Phys. Rev. Lett.* **37**, 36.
Rice, M. J. (1978). Proc. Int. Conf. on Quasi-one-dimensional Conductors, Dubrovnik 1978, Lecture Notes in Physics, Vol. 96 (Eds S. Barisic *et al.*), p. 230 (Springer: Berlin).
Rice, M. J., Duke, C. B., and Lipari, N. O. (1975). *Solid State Commun.* **17**, 1089.
Rice, M. J., Pietronero, L., and Bruesch, P. (1977). *Solid State Commun.* **21**, 757.
Tanner, D. B., Jacobsen, C. S., Bright, A. A., and Heeger, A. J. (1977). *Phys. Rev.* B **16**, 3283.

Manuscript received 25 May, accepted 1 December 1988